

Impacts of projected climate change on the thermodynamics of a shallow and a deep lake in Finland: model simulations and Bayesian uncertainty analysis

Tuomo M. Saloranta, Martin Forsius, Marko Järvinen and Lauri Arvola

ABSTRACT

A lake model (MyLake) has been used to simulate the impacts of the projected future (2071–2100) climate on the thermodynamic properties of a shallow and a deep lake in Finland. The model has been calibrated using a Bayesian Markov chain Monte Carlo (MCMC) simulation method. The model results show, among others, that the largest change in water temperature in a projected future climate occurs in April–May when a 4.6–7.6°C increase in epilimnion and 2.7–4.4°C increase in whole-lake monthly mean temperature occurs compared to the climate of 1961–1990. This corresponds to a large decrease in the probability of ice cover in March–April. In winter and early spring a negative correlation was obtained between lake water and air temperatures in a projected future climate due to the thermal buffering feature of the lake ice and snow cover. The uncertainties connected to the choice of the general circulation model and the boundary condition forcing for the regional atmospheric climate model were often significantly larger than the uncertainties connected to MyLake model parameter values.

Key words | climate change, lake thermodynamics, Markov chain Monte Carlo, modelling

Tuomo M. Saloranta (corresponding author)
Norwegian Institute for Water Research (NIVA),
Gaustadalléen 21, Oslo N-0349,
Norway
Tel.: +47 9916 4559
Fax: +47 2218 5200
E-mail: tuomo.saloranta@niva.no

Martin Forsius
Marko Järvinen
Finnish Environment Institute (SYKE),
PO Box 140, Helsinki FI-00251,
Finland

Lauri Arvola
Lammi Biological Station,
University of Helsinki,
Pääjärventie 320, Lammi FI-16900,
Finland

INTRODUCTION

Lakes are more and more experiencing the consequences of the changing climate (Blenckner 2005; Blenckner *et al.* 2007). Long term changes in weather patterns (temperature, precipitation, wind speed, solar radiation, etc) have a direct impact on the lake water temperature, stratification and light conditions, and also an indirect impact via the lake catchment. The response of lakes to increasing air temperatures depends on the lake type. In shallow, polymictic lakes, the entire water column can respond to fluctuations in air temperature, while in thermally stratified lakes the increased thermal stability can effectively shield the hypolimnion from the effects of the increasing air temperature. This effect is particularly pronounced in small, highly coloured lakes (such as Lake Valkea-Kotinen in this paper) where the surface layer can warm up quickly and remain extremely shallow, and where water clarity can be an important regulator of thermal stratification and also

have a major effect on the underwater light climate and, therefore, the ecology of the lake (Salonen *et al.* 1984). In thermally stratified lakes, increasing air temperatures will only result in increasing hypolimnetic temperatures if winds are strong enough to result in mixing (sometimes mediated by internal waves) between the stratified layer and the hypolimnion.

Moreover, in colder regions where lake ice and snow cover is formed, lakes may show a particularly sensitive and nonlinear response to changes in climate, owing to the discontinuities in water behaviour both at 0°C (ice freezing/melting) and at 4°C (density maximum of fresh water), and to the fact that ice and snow cover effectively hamper fluxes of light, heat, matter and momentum between the atmosphere and the water column. Thus a projected climate change may have an especially profound impact on the chemistry and ecosystems in lakes of colder

doi: 10.2166/nh.2009.030

regions (e.g. Livingstone & Dokulil 2001; Järvinen *et al.* 2002; Vähätalo *et al.* 2003).

Since lakes are complicated systems, numerical models are often applied to simulate the impacts of climate change on lakes. Model applications with seasonal lake ice cover have been evaluated by Fang & Stefan (1998), Hostetler & Small (1999) and Blenckner *et al.* (2002). The obvious advantage of numerical models is their capability to holistically represent the lake system and synthesize knowledge on the different lake subsystems, such as ice cover, water dynamics and thermodynamics, sediment–water interaction, chemistry and biology. With models one can also explore the consequences of new future events unseen in the historical time series. However, the inherent uncertainties connected to such model simulation results are seldom quantified, despite the fact that knowledge of uncertainties is an important element in, for example, decision-making concerning the environmental lake management (Saloranta *et al.* 2003). Failure to account for uncertainties in model results could mean that misleading model results are provided to environmental managers and decision-makers. This may further lead to wrong management decisions on the often costly lake management measures, e.g. connected to mitigation of the impacts of climate change (Arhonditsis *et al.* 2007; Blenckner 2008).

In this paper, the lake model code MyLake (Saloranta & Andersen 2007) is used to simulate the impacts of the projected future climate on the thermodynamic properties of two humic lakes in Finland: one small and shallow (Valkea-Kotinen) and one larger and deeper lake (Pääjärvi). Lake Valkea-Kotinen and its catchment has been the subject of much biogeochemical and limnological research (Forsius *et al.* 1995; Keskitalo *et al.* 1998; Vähätalo *et al.* 2000, 2003; Starr & Ukonmaahano 2001, 2004; Holmberg *et al.* 2006), while in Pääjärvi potential impacts of climatic variation have been studied by analysing long-term limnological data against meteorological data and climate indices (e.g. NAO) (Järvinen *et al.* 2002, 2006; Blenckner *et al.* 2004, 2007; George *et al.* 2004).

One of the main aims in this paper is to take properly into account uncertainties in the model simulation results. Therefore we calibrate the model and estimate its parameter uncertainties using the Markov chain Monte

Carlo (MCMC) simulation method (e.g. Gamerman 1999) and time series of water temperature for the period 2000–2002. The estimated model parameter uncertainties are then taken into account and presented as confidence intervals in the simulation results for present (1961–1990) and future (2071–2100) “lake water climate” (i.e. water temperature, stratification, ice and snow cover) in the two case study lakes. The MCMC method, based on Bayesian inference, has several advantages over manual calibration and basic Monte Carlo uncertainty analysis methods (e.g. Kuczera & Parent 1998; Arhonditsis *et al.* 2007; Saloranta *et al.* 2008), in that probability distributions of model parameter values (which can be multimodal) as well as correlations between the parameters can be investigated using this method (i.e. a joint probability density function of all estimated parameters is simulated). In the MCMC simulation parameter combinations which produce improbable model results, compared to observations and their error variances, are disregarded.

METHODS

Site description and model application

Two lakes have been studied and modelled as part of the research, these being Lake Valkea-Kotinen and Lake Pääjärvi. These are two very different type of lakes situated 35 km from each other in the Lammi region in southern Finland, about 130 km north of the city of Helsinki. Valkea-Kotinen is a small humic forest lake with a surface area of 0.04 km² and maximum depth of about 7 m (Rask *et al.* 1998), while Pääjärvi is a larger and deeper lake with a surface area of 13 km² and maximum depth of about 85 m (Kankaala *et al.* 1996). Bottom depth distributions in the lakes are shown in Figure 1. Time series of temperature profiles exist from both lakes and the lake ice and nearby snow cover thicknesses as well as ice cover freezing and melting dates are also recorded. For the MyLake calibration and parameter uncertainty analysis (MCMC simulation) temperature time series data from three different depth levels are used (0.5, 2 and 4.5 m in Valkea-Kotinen and 1, 7.5 and 40 m in Pääjärvi). These levels represent epi-, meta- and hypolimnion, i.e. the well-mixed surface layer above the

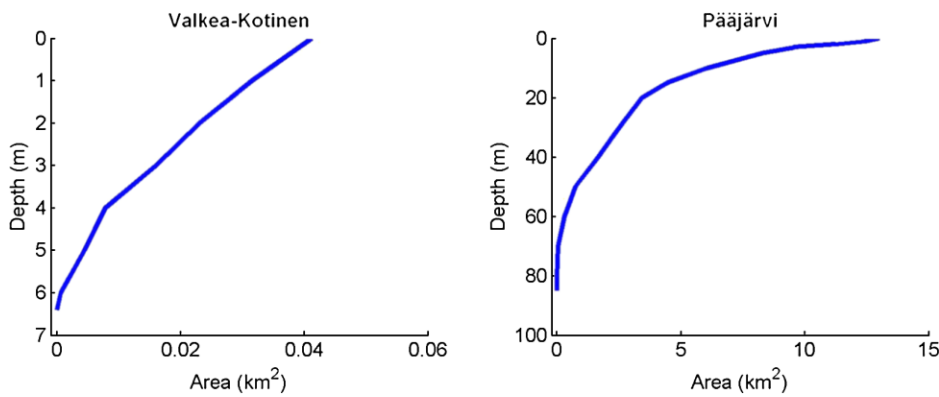


Figure 1 | The horizontal water area versus depth in lakes Valkea-Kotinen and Pääjärvi.

pycnocline, the most stratified layer around the pycnocline and the deeper water column below the pycnocline, respectively.

The MyLake model code (Multi-year Lake simulation model; Saloranta & Andersen 2007), which has been applied in the study to simulate the impacts of projected future climate on the thermodynamic lake properties, is a one-dimensional process-based model code which aims to combine good simulation capabilities with efficient model execution time and easy application of numerical uncertainty and sensitivity analysis techniques. Moreover, the basic idea behind the MyLake model code development has been to include only the most significant physical, chemical and biological processes in a well-balanced and robust way. In addition to the basic lake thermodynamic variables, such as daily evolution of temperature and density profiles as well as of ice and snow cover, MyLake is able to simulate also some basic water quality variables (e.g. phosphorus, chlorophyll, suspended matter).

In the MyLake model the following heat conservation equation is solved for the temperature distribution in a horizontally homogeneous, vertically stratified lake:

$$A \frac{\partial T}{\partial t} = \frac{\partial}{\partial z} \left[KA \frac{\partial T}{\partial z} \right] + A \frac{Q^*}{\rho_w C_p} \quad (1)$$

where the first right-hand side term represents diffusive mixing processes and the second term local heating (due to turbulent, long-wave, solar radiation and sediment heat fluxes), and where temperature T [°C], vertical diffusion coefficient K [$\text{m}^2 \text{d}^{-1}$] and local heating rate Q^* [$\text{J m}^{-3} \text{d}^{-1}$] are all functions of depth z and time t , while area A [m^2]

is a function of depth alone. Temperature and heat are related through the specific heat capacity of water C_p [$\text{J kg}^{-1} \text{°C}^{-1}$] and the density of water ρ_w [kg m^{-3}]. Following Hondzo & Stefan (1993), the vertical diffusion coefficient K is calculated on the basis of the stability frequency $N^2 = (g/\rho_w)(\partial\rho_w/\partial z)$ [s^{-2}]:

$$K = a_k (N^2)^{-0.43} \quad (2)$$

and the total kinetic energy E_{kin} [J] available for wind-induced mixing in open water period accumulated over one model time step Δt is calculated by

$$E_{kin} = W_{str} A_s \sqrt{\frac{\tau^3}{\rho_w}} \Delta t \quad (3)$$

where τ is wind stress [N m^{-2}]. The coefficients a_k and W_{str} are parametrized by lake surface area A_s [km^2]:

$$a_k = 0.00706 (A_s)^{0.56} \quad (4)$$

(in open water period; constant value applied under ice)

$$W_{str} = 1.0 - \exp(-0.3A_s) \quad (5)$$

The vertical resolution in the model is user-definable, while the time step in the model is fixed at 24 h, except for the calculation of temperature profile and convection which are calculated twice a day, both at day and night. In order to calculate the radiative and turbulent heat fluxes, water surface albedo, surface wind stress or astronomical variables the MATLAB Air-Sea Toolbox (<http://woodshole.er.usgs.gov/operations/sea-mat/>) has been used.

When water layer temperatures below freezing point are encountered, ice formation is initiated. The compaction of snow, affecting its density and thermal conductivity, as well as snow ice formation are taken into account in calculating the total ice thickness. A more detailed description of the model code with technical details and equations is given in Saloranta & Andersen (2007). For previous MyLake model applications see Kankaala *et al.* (2006), Saloranta (2006) and Saloranta & Andersen (2007).

Time series based on interpolation of synoptic weather station observations were used as meteorological forcing for both lakes in the MCMC simulations, while simulated time series from a regional atmospheric climate model (RCAO) were used in simulations of the present and future climate (see the next section). In addition, observed and simulated time series (2000–2002) of runoff and river water discharge were used as hydrological forcing in the MCMC simulations. These three-year time series were simply repeated to construct 30-year time series for the simulations of present and future climate, implying that no changes in the volumes of the water discharges are taken into account in the future climate scenarios. However, since the effect of surface discharge on the lake temperature is probably small due to the relatively long water residence times in Valkea-Kotinen (about 2 years) and Pääjärvi (about 4 years), this assumption seems to be justified. Groundwater inflow to Valkea-Kotinen might contribute to shorter water residence time than estimated above, but there is little knowledge of the magnitude of this flow. The daily temperature in the surface discharge was in all model simulations estimated by a 5-d running mean of the air temperature (truncated for temperatures $< 0^{\circ}\text{C}$), i.e. a mean of the particular day and the four preceding days. All model simulations were started in May and observed temperature profiles in May 2000 were used as initial conditions in the MCMC simulations. In simulations with the RCAO model forcing a homogeneous initial temperature profile at 4°C was assumed, and the first (half) simulation year was regarded as a “spin-up” year and thus discarded from further analysis of the model results.

Meteorological forcing for present and future climate

The majority of the daily meteorological forcing time series for the MyLake model in the MCMC simulations

(i.e. model calibration and uncertainty analysis) in Valkea-Kotinen and Pääjärvi in 2000–2002 were obtained from a gridded meteorological database interpolated from all available synoptic weather stations. This database is provided by the Baltic Sea Experiment Hydrological Data Centre (BHDC) hosted by the Swedish Meteorological and Hydrological Institute (SMHI). From the BHDC data a grid point was extracted, representing the Lammi region in the vicinity of the study lakes (grid point coordinates are 61.5N, 25.5E; those of Valkea-Kotinen are 61.14N, 25.04E). Cloudiness was missing in the BHDC data and it was supplemented with observations from the meteorological station in Jokioinen, about 100 km south-west of Lammi.

The daily meteorological time series representing a future projected climate (2071–2100) and the climate control period (1961–1990) in the Lammi region were obtained from a regional climate model (RCAO model, Rossby Center, Sweden (Jones *et al.* 2004; Räisänen *et al.* 2004)). Two different global general circulation models (GCMs), ECHAM4 and HadAM3, were used to provide the lateral atmospheric boundary condition forcing for the RCAO model. Furthermore, two different greenhouse gas emission scenarios, A2 and B2 (IPCC 2001; generally less greenhouse gas emissions in the B2 than in the A2 scenario) were used in RCAO model simulations. Thus, six different 30-year RCAO model simulations are used as climate forcing in the study, corresponding to the control period, A2 and B2 scenarios, and the two different GCMs. Figure 2 shows the RCAO model simulated changes in air temperature and wind speed in 2071–2100 compared to the control period 1961–1990. For example, in the A2 scenario with ECHAM4 forcing the mean air temperature has increased by 5°C and wind speed by 8% in the Lammi region.

In order to find out how representative the RCAO model results for the control period (1961–1990) are for the Lammi region a comparison was made for six different meteorological parameters between observations from Jokioinen (since no comprehensive meteorological data exist from Lammi for the period 1961–1990) and two different sets of control period results from the RCAO model, corresponding to the ECHAM4 and HadAM3 forcings. In addition, time series from the Lammi

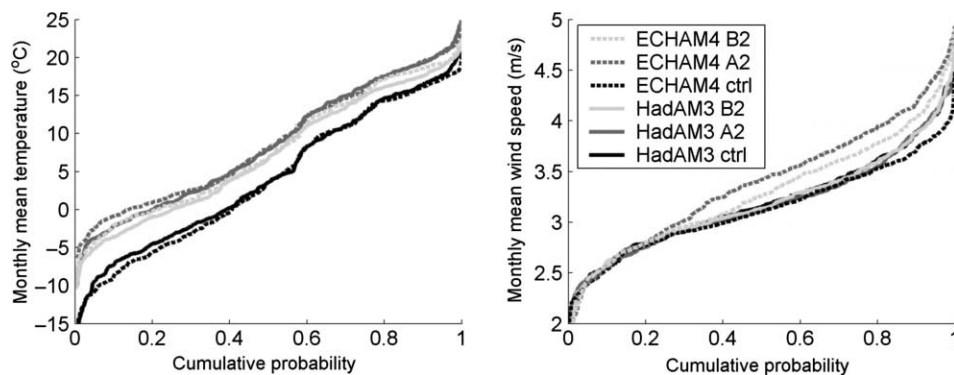


Figure 2 | The RCAO model simulated changes in mean monthly (a) air temperature and (b) wind speed in scenarios A2 and B2 in 2071–2100 compared to the control period 1961–1990. ECHAM4 and HadAM3 refer to the two different general circulation models used as boundary condition forcing for the RCAO model.

meteorological station starting in the mid-1960s were used in these comparisons. Medians, and 10th and 90th percentiles of the 30 years of data were studied in the comparison exercise. Compared to the observed time series at Jokioinen for the same 1961–1990 period, the RCAO model control period results with the HadAM3 and ECHAM4 forcings show the following (unless otherwise stated, the following values represent medians of the 30 yearly mean or sum values):

- an underestimation for the yearly mean global radiation (by 1.3 and 2.1 MJ m⁻² d⁻¹ for HadAM3 and ECHAM4 forcings, respectively),
- a relatively large overestimation for the yearly sum of precipitation (by 191 and 315 mm yr⁻¹ for HadAM3 and ECHAM4 forcings, respectively),
- an underestimation for the yearly mean wind speed (by 0.5 and 0.6 m s⁻¹ for HadAM3 and ECHAM4 forcings, respectively),
- a rather good fit for the yearly mean temperature (slight over- and underestimation by 0.4 and 0.1°C for HadAM3 and ECHAM4 forcings, respectively; the difference for the 10th and 90th percentiles is about ± 1°C),
- a rather good fit for the yearly mean relative humidity (a slight overestimation by 2 and 4% units for HadAM3 and ECHAM4 forcings, respectively),
- an overestimation for the yearly mean cloudiness (by 0.10 and 0.13 for HadAM3 and ECHAM4 forcings, respectively).

Furthermore, the comparison showed that the Jokioinen station represents quite well the Lammi station for

temperature and rainfall, whereas relative humidity and cloudiness are somewhat higher at Jokioinen. Wind speed and global radiation were not measured at the Lammi meteorological station.

Model calibration and uncertainty analysis

In order to estimate and express model parameter values in terms of probability distributions, rather than single values, we applied the MCMC simulation method. This method is based on Bayesian inference and is suitable for automatic model calibration and estimation of proper parameter uncertainties, and thus uncertainties in prediction results in the current model application. The application of MCMC simulation methods in numerical lake modelling is still rather limited but is anticipated to increase due to the significant advantages of the method for many types of model applications (Kuczera & Parent 1998; Malve *et al.* 2005, 2007; Larssen *et al.* 2006; Arhonditsis *et al.* 2007; Saloranta *et al.* 2008).

The general idea of MCMC simulation is based on a “guided” random walk in the parameter space. A large number of iterations (i.e. model runs) are executed and after the chain of these random “steps” in the parameter space has properly converged, it represents samples of parameter sets which optimally, in a probabilistic sense, fit the corresponding model results to the observations used in the calibration. In other words, the chain represents samples from the posterior joint probability distribution of all the estimated parameters. Thus the parameter

unidentifiability (or equifinality) problem (Beven 2006), which is that several different parameter value combinations can produce similar simulation results, can be resolved and represented in the MCMC simulation.

Before the actual MCMC simulation is started, so-called prior distributions are defined, reflecting the previous knowledge (or lack of it) on the probability of different parameter values. In each iteration round in the MCMC simulation, a likelihood measure L is calculated for the M observations T^{obs} (temperature), given the corresponding M model results T^{mod} simulated with currently selected parameter values:

$$L \propto \frac{1}{\prod_{i=1}^M \sigma_i} \exp\left(-\sum_{i=1}^M \frac{1}{2\sigma_i^2} (T_i^{obs} - T_i^{mod})^2\right) \quad (6)$$

where σ^2 is the error variance of T^{obs} . This accounts for spatial (within the lake) and temporal (during a day) variability of observed *in situ* water temperatures around the daily mean value for the whole lake at a certain depth level, which the model results are assumed to represent. Since little is known about the exact distributional form of this small scale variability, the assumption has been made that these spatio-temporal deviations from the mean value are normal distributed, as expressed in Equation (6). Figure 3 shows a graphical illustration of the Bayesian model assumed in our MCMC simulations.

A common standard deviation is assumed for each of the three depth levels which are considered in our MCMC simulations. The distributions are estimated by an MCMC technique called Gibbs sampling (e.g. Gamerman 1999). For estimation of the four calibration coefficients (a_1 – a_4 ; see below) an adaptive Metropolis MCMC technique (Haario *et al.* 2001) is utilized. In this technique, an accept/reject procedure, based on comparison of the product of L and the parameter joint prior probability from the current and preceding iteration rounds, together with the covariance adaptation method, finally guides the parameter chain to the correct posterior joint distribution. More details on these MCMC techniques can be found, for example, in Gamerman (1999), Gelman *et al.* (2004) and Larssen *et al.* (2006).

On the basis of model sensitivity analysis (Extended FAST method; Saltelli *et al.* 2000; Saloranta & Andersen

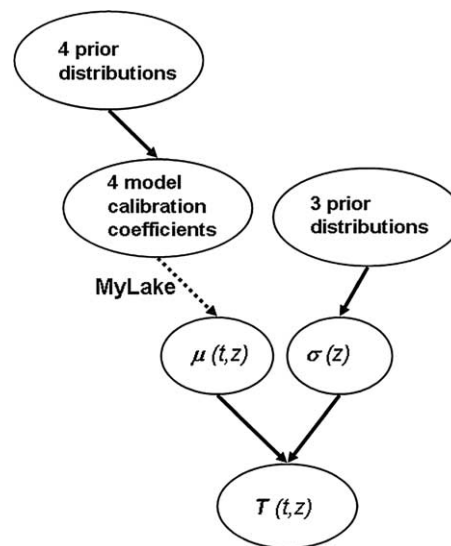


Figure 3 | Graphical illustration of the Bayesian model assumed in the MCMC simulation. The water temperature observations at a particular time and depth $T(t, z)$ in the lake are assumed to be normal distributed with a mean μ (separate μ for each time and depth) and a standard deviation σ (assumed time-invariant, but separate σ for each of the three selected depth levels), as expressed in the likelihood function in Equation (6). Both μ and σ are unknown random variables whose distributions are estimated in the MCMC simulation (the solid arrows denote stochastic relationships). The daily mean lake temperature profile (i.e. the μ) can be simulated by the MyLake model, and thus there is a deterministic link (denoted by a dashed arrow) between the four model calibration coefficients a_1 – a_4 and the μ . Consequently, instead of estimating the distributions of μ directly we estimate distributions of a_1 – a_4 . Finally, our prior knowledge (or lack of that) on the distributions of a_1 – a_4 and σ are expressed in the prior distributions (see Table 1).

2007) four key model parameters were selected to be estimated in the MCMC simulations. These key parameters are: (1) effective lake surface area A_{eff} (affecting the available wind mixing energy, and hypolimnetic turbulent diffusion coefficient K), (2) light attenuation coefficient in water ϵ , (3) minimum allowed value of Brunt-Väisälä frequency N_{min}^2 (determining the maximum possible value of K) and (4) melting snow and ice albedos α_s , α_i .

In the MCMC simulations these key parameters are represented by four calibration coefficients a_1 – a_4 . Table 1 shows the relations of the four calibration coefficients to the key model parameters. The prior distributions of a_1 – a_2 (see Table 1) were based on expert judgement, that of a_3 on some previous observations of ϵ and that of a_4 on published values of α_s and α_i (Perovich 1998; Henneman & Stefan 1999; Leppäranta *et al.* 2003). Prior distributions of σ_1 – σ_3 were assumed to be flat non-informative distributions.

Table 1 | Prior probability distribution functions (PDFs) for the four parameter calibration coefficients (a_1 – a_4) and for the three standard deviations (σ_1 – σ_3) estimated in the MCMC simulation. The relation of the calibration coefficients to the actual model parameter values is shown in the last column. Parameter abbreviations are explained in the main text. SD denotes standard deviation and CF denotes confidence factor in lognormal distributions, so that 95% of the values are within a factor CF around the median. Asterisks (*) denote nominal model parameter values

Coeff.	Prior PDF type	Parameters of PDF	Relation to model parameters
a_1	lognormal	1, 10 (median, CF)	$A_{eff} = a_1 \cdot A_s$
a_2	lognormal	1, 10 (median, CF)	$N_{min}^2 = a_2 \cdot N_{min}^{2*}$
a_3	normal	2.5, 0.5 (mean, SD for Valkea-Kotinen)	$\varepsilon = a_3$
		0.9, 0.5 (mean, SD for Pääjärvi)	
a_4	normal	0.35, 0.1 (mean, SD)	$\alpha_i = a_4, \alpha_s = a_4 + 0.15$
$\sigma_1 - \sigma_3$	gamma, for precision $\tau = 1/\sigma^2$ (a non-informative prior)	0.001, 0.001 (rate, shape)	$\sigma_1^2 - \sigma_3^2$ are the error variances of the temperature at depths $z_1 - z_3$ (see Equation (6))

The values of those model parameters not estimated in the MCMC simulation were fixed at their nominal values. In order to reduce the autocovariance in the observed temperature time series T^{obs} , these were thinned so that only every 15th sample was used in calculating L (resulting in about 40 observations used from each depth in the calibration period 2000–2002).

RESULTS

Model calibration and uncertainty analysis

In order to assess the convergence of the parameter chains, three parallel chains were simulated with different starting points (20th, 50th and 80th percentiles of the corresponding prior distributions of a_1 – a_4) and a convergence measure R was calculated (Gelman *et al.* 2004), based on the comparison of variances between and within the three chains. The total length of each chain was 3,000 iterations and the first halves of the chains were discarded as the burn-in period. Convergence was tested on the remaining 1,500 iterations and the chains seemed to have converged well as $R < 1.02$. Finally, the three converged chains were joined to form our final parameter chain (shown in Figure 4 for Valkea-Kotinen). The percentage of accepted proposal steps in the final converged chain was 23 and 19% for Valkea-Kotinen and Pääjärvi, respectively. The only stronger ($|r| > 0.5$) correlations were found between a_1 and a_3

($r = 0.82$) in Valkea-Kotinen and between a_1 and a_2 ($r = 0.67$) in Pääjärvi, indicating that a larger (smaller) A_{eff} must be accompanied by a larger (smaller) ε in Valkea-Kotinen, and by a smaller (larger) maximum possible value of K in Pääjärvi, in order to give reasonable temperature simulations. The final model simulations with uncertainty bounds, shown in Figures 5 and 6, both with present and future climate's meteorological forcing, are generated by randomly drawing 200 samples of parameter sets from these joint chains (separate chains for Valkea-Kotinen and Pääjärvi) and conducting 200 simulations with these different parameter sets, with each particular meteorological forcing.

Figure 5 shows that the model is well calibrated in the MCMC simulations and the estimated prediction uncertainty bounds seem to be consistent with the variation in the temperature observations. The median model bias compared to observations in the 200 simulations was in Valkea-Kotinen -0.7°C for the 0.5 m depth, -0.6°C for the 2 m depth and -0.3°C for the 4.5 m depth, and in Pääjärvi practically no bias ($< 0.02^\circ\text{C}$) for the 1 and 40 m depths and 0.4°C for the 7.5 m depth. The posterior distributions (shown in Figure 4 for Valkea-Kotinen) are all different from their prior distributions, indicating that the distributions of a_1 – a_4 (and thus the related key model parameters, see Table 1) and σ_1 – σ_3 were well updated during the MCMC simulation on the basis of the temperature data used. The median values of the posterior distributions for

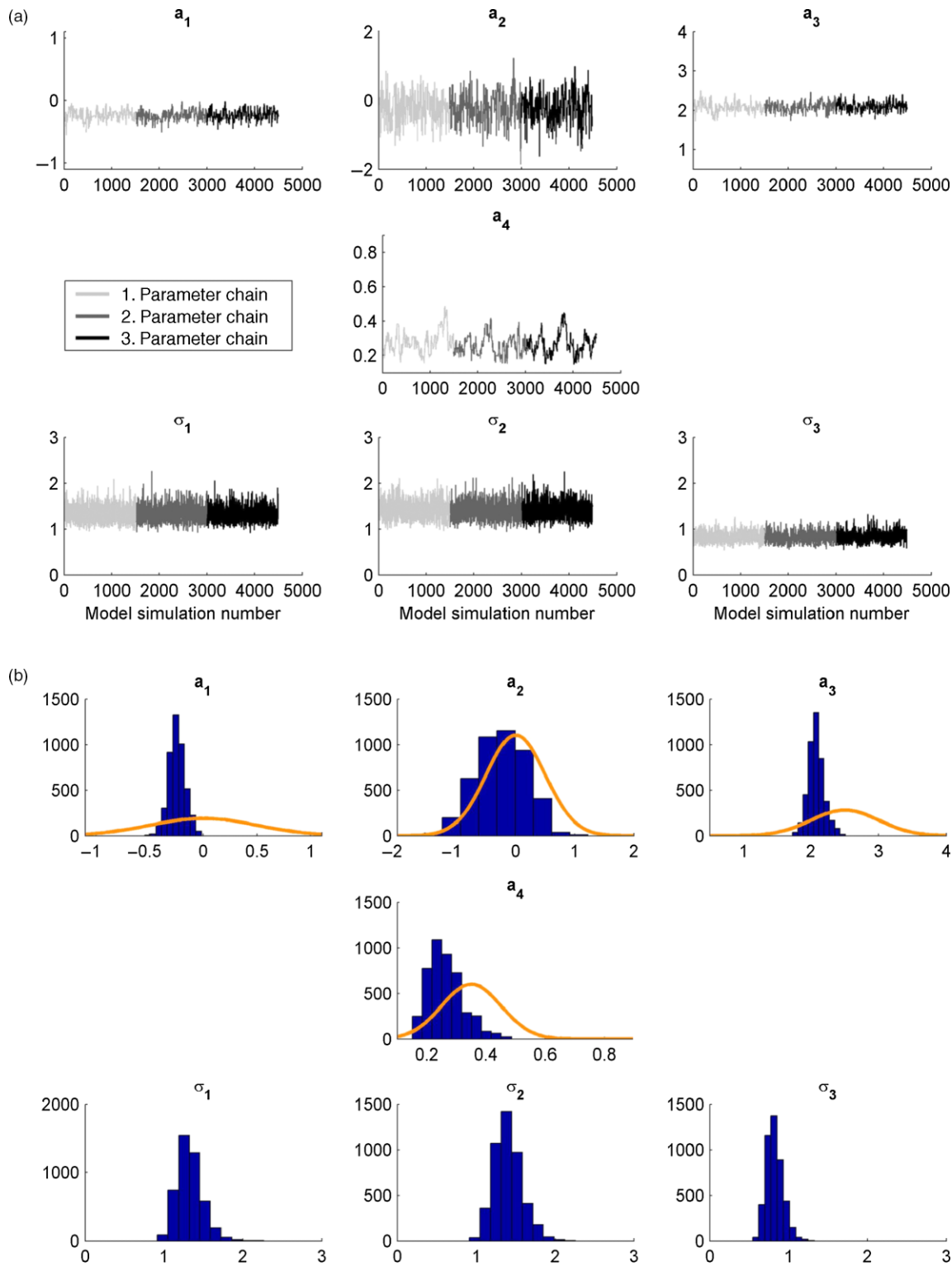


Figure 4 | (a) Converged parameter chains and (b) histograms based on these chain values (i.e. posterior probability distributions) for the four parameter calibration coefficients (a_1 – a_4) and for the three standard deviations (σ_1 – σ_3) estimated in the MCMC simulation for Valkea-Kotinen. Prior probability distributions are also shown, except for σ_1 – σ_3 for which non-informative priors are used. Note that the y axis in (a) and x axis in (b) of a_1 – a_2 are \log_{10} -transformed.

a_1 – a_4 were 0.57, 0.59, 2.07 and 0.26 for Valkea-Kotinen and 0.27, 0.41, 1.55 and 0.45 for Pääjärvi. Moreover the posterior distributions of a_1 and a_4 (related to A_{eff} , and α_s and α_i) were significantly narrower in Pääjärvi than in Valkea-Kotinen, and that of a_3 (related to ε) significantly narrower in Valkea-Kotinen than in Pääjärvi.

The predicted ice freezing dates in Valkea-Kotinen and melting dates in both lakes also fit well with corresponding observations (not used in calibration); the difference between observations and the simulated 90% credible intervals is -2 to 3 d. In Pääjärvi there is a significant spatial variability in the time of formation of initial ice cover, which the one-dimensional model cannot reproduce. Consequently, it was not possible to compare the recorded ice freezing dates in Pääjärvi with the model results. The model simulations of the seasonal evolution of the ice and snow cover (water equivalent) thickness were in good agreement with observations (not shown); the difference between the simulated and observed maximum ice thickness in 2000–2002 (~ 0.4 m) was only a few centimetres in both lakes.

The model evaluation results (Figure 5) showed that the calibrated model simulates well the 2000–2002 seasonal evolution of the thermodynamic properties in the case study lakes and produces reasonable confidence intervals for these results (Figure 4). This increases confidence in that the model can be successfully used to simulate the impacts of the projected climate change on these lakes. Potential methodological model uncertainties are discussed in more details in the last section.

Simulations with future climate forcing scenarios

In order to simulate the impacts of the projected climate change, the results from the RCAO model, with both the HadAM3 and ECHAM4 forcings, were used as forcings for the calibrated MyLake model in Valkea-Kotinen and Pääjärvi. Simulations were run both for the control period (1961–1990) and for the projected future climate (2071–2100), and monthly means were calculated from these 29-year long time series (the first “spin-up” years 1961 and 2071 are neglected). Figure 6 shows the climate scenario simulation results for ice cover probability and mean temperature in both lakes. These and other relevant

simulation results are discussed in more detail in the following two subsections.

Valkea-Kotinen

The A2 scenario simulation results for Valkea-Kotinen (Figure 6(a)) show that the whole-lake monthly mean temperature increased in April–October by 1.4–4.4°C compared to the control period (all such value intervals in this and the following subsection correspond to the minimum and maximum of the 90% credibility intervals of the results with HadAM3 and ECHAM4 forcings), the largest increase being in April, corresponding to the large decrease in the probability of ice cover in March–April. A similar larger drop in the probability of ice cover is also seen in November. The mean length of the ice covered period is shortened by 56–89 d. The simulated water temperature increase (not shown) is largest in the epilimnion (0.5 m depth), being 4.6–6.1 and 3.5–4.6°C higher in April and May, respectively, in the A2 scenario compared to the control period. Similarly, in June–November the simulated epilimnion temperature in the A2 scenario is 1.9–3.8°C higher, while in December–February it is almost the same ($< 0.45^\circ\text{C}$ difference), compared to the control period. In the hypolimnion (4.5 m depth) the simulated difference between the A2 scenario and control period is largest in April and October (1.2–2.6°C difference) and smallest in December–February ($< 0.4^\circ\text{C}$ difference).

The simulated mean monthly pycnocline depth (closely related to thermocline depth; calculated as density gradient weighed mean of the depth) is only calculated when a density gradient $> 0.1 \text{ kg m}^{-3}$ per metre exists somewhere in the water column over 50% of the days of a month in all 29 years. The simulated mean monthly pycnocline depth increases from 1 to 3 m in May–September in the control scenario and does not seem to undergo very dramatic changes in the projected future climate as the pycnocline is at its largest 0.10–0.43 m deeper in May and 0.05–0.47 m shallower in September (A2 scenario) compared to the control period.

The simulations with ECHAM4 forcing show generally slightly larger changes than those with HadAM3 forcing, and similarly the changes in the A2 scenarios are obviously larger compared to the B2 scenarios. However, the general pattern of change is much the same in all these scenarios.

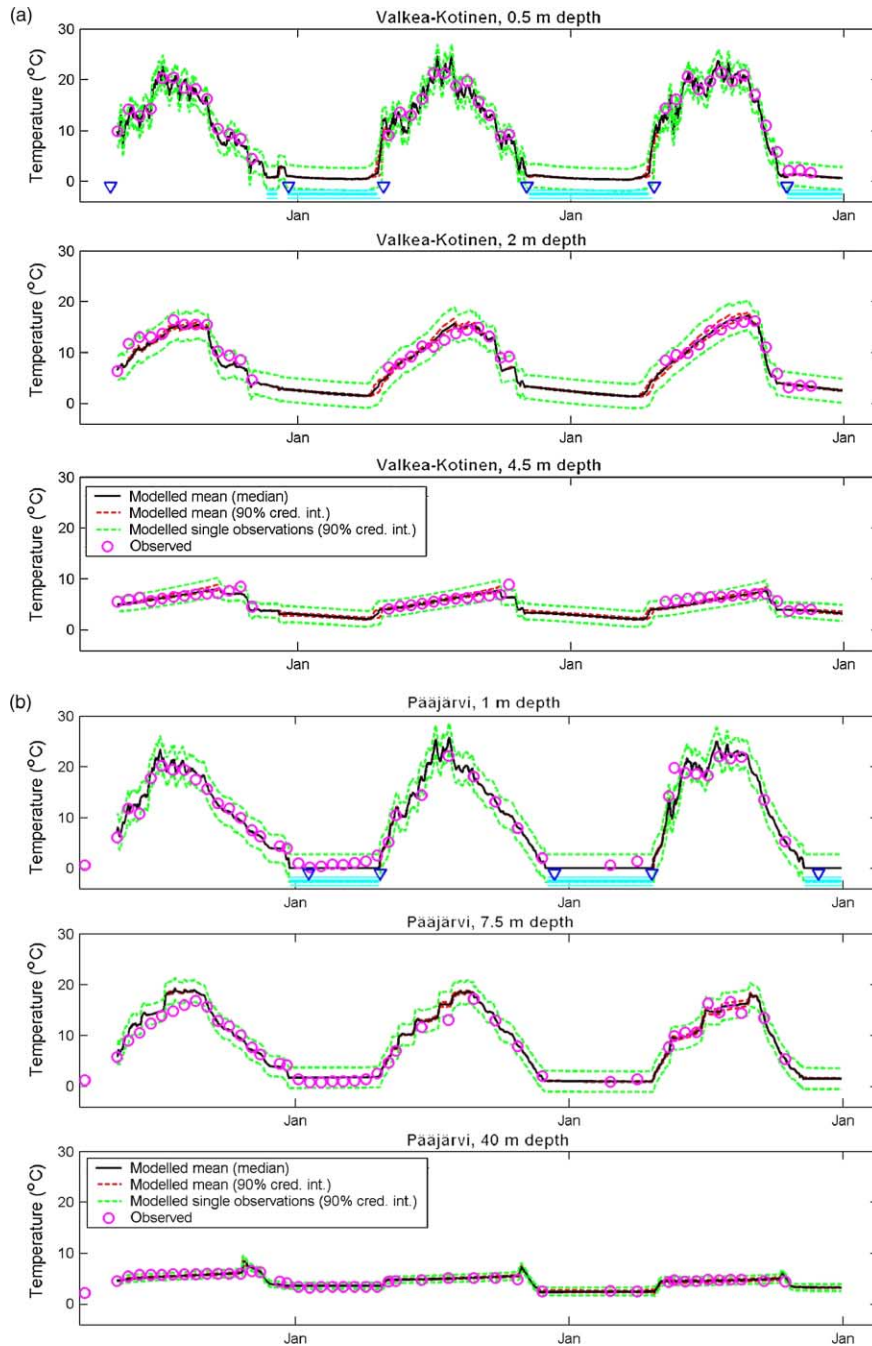


Figure 5 | Calibrated model results (May 2000–December 2002) vs. observations of temperature in (a) Valkea-Kotinen and (b) Pääjärvi. Dark (black) solid line shows median of the simulated mean lake temperature (i.e. μ in Figure 3) and dark (red) dashed lines its 90% credible interval, based on the 200 simulations conducted in the uncertainty analysis, where parameter values sets were resampled from the parameter chains estimated in the MCMC simulation. Light (green) dashed lines show the simulated 90% credible interval for individual observations (i.e. ± 1.65 times the median of standard deviations σ_1 – σ_3 around mean lake temperature μ). The horizontal lines in the upper panel show the simulated median (thick line) and 90% credible intervals (thin lines) of the presence of ice cover, based on the 200 simulations conducted in the uncertainty analysis. The triangle markers point at the observed days of first complete ice cover and final melting. Note that due to the assumption of time-invariant σ_1 – σ_3 , estimated mostly on the basis of the data from the open water season, some of the credible intervals for individual observations include slightly negative temperatures in winter when the water temperature is near zero.

Pääjärvi

The A2 scenario simulation results for Pääjärvi (Figure 6(b)) show that whole-lake monthly mean temperature increased in April–December by 1.0–3.6°C compared to the control period, the largest increase being in May, corresponding to the large decrease in the probability of ice cover in April (–0.7 to –0.9). A similar larger drop in the probability of ice cover is also seen in December. The mean length of the ice covered period is shortened by 68–101 d. The simulated water temperature increase (not shown) is largest in the epilimnion (1 m depth), being 6.6–7.6°C higher in May in the A2 scenario compared to the control period. Similarly, in April and in June–December the simulated epilimnion temperature in the A2 scenario is 2.4–3.8°C higher, while in January–March it is almost the same (<0.9°C difference), compared to the control period. In the hypolimnion (40 m depth) the simulated difference between the A2 scenario and the control period is largest in November (1.8–2.3°C difference), otherwise smaller (<1.2°C difference), showing even some cooling, especially in January–March in the simulations with the ECHAM4 forcing.

The simulated mean monthly pycnocline depth increases from 5 to 15 m in June–September in the control scenario and is at its largest 0.15–1.0 m deeper in June and 1.1–2.9 m shallower in September in the projected future climate (A2 scenario) compared to the control period.

As in simulations for Valkea-Kotinen, the simulations for Pääjärvi with the ECHAM4 forcing and A2 scenario show generally slightly larger changes than with the HadAM3 forcing and B2 scenario, but the general pattern of change remains much the same in all these scenarios.

DISCUSSION AND CONCLUSIONS

The approach of calibrating the MyLake model and analyzing its parameter uncertainties with the MCMC simulation method worked well and produced consistent results both when comparing the simulated seasonal evolution of the lake water temperature and ice cover to corresponding observations, and when considering the reasonability of the simulated posterior probability distributions of the model parameters (including correlation information between the different parameters). Albedo is

the main parameter affecting the melting rate of the snow and ice cover, and the posterior distributions of α_s and α_i values may therefore also incorporate effects of rainfall on snow albedo as well as disintegration of ice crystals in the late melting season, which are processes not explicitly represented in the MyLake model code. The lower α_s and α_i values estimated for Valkea-Kotinen than for Pääjärvi might be due to the larger transport of organic matter (e.g. pine needles) from the surrounding forest onto the melting ice and snow surface of this small lake.

Since the model is well calibrated and the model parameter uncertainties properly taken into account, there is increased confidence using these parameter distributions to express technical model uncertainties (i.e. uncertainties connected to model parameter values (Funtowicz & Ravetz 1990; Saloranta *et al.* 2003)) in simulations of lake thermodynamics in a projected future climate. As indicated in Figure 6, uncertainties connected to the choice of the GCM (ECHAM4 or HadAM3) used as boundary condition forcing for the RCAO model are often larger than the uncertainties connected to MyLake model parameter values estimated in the MCMC simulations.

In the simulations it has been assumed that the estimated distributions of the key model parameters (A_{eff} , ε , N_{min}^2 , α_s , α_i) do not change significantly in a future climate. In other words, only the atmospheric forcing (i.e. global radiation, air temperature, wind speed, cloudiness, humidity, snow fall) can have a major shift in a future climate in the simulations. This assumption seems reasonable, at least for the parameters A_{eff} and N_{min}^2 which are more connected to the basic lake geometry and mixing dynamics. Water clarity (and thus ε) and the albedos of melting snow and ice might systematically increase or decrease in the future. Water clarity in the study lakes is related to dissolved organic carbon (DOC) concentration, which can change due to long-term combined effects of decreasing atmospheric sulfate deposition and changes in climate (Holmberg *et al.* 2006; Monteith *et al.* 2007; Futter *et al.* 2009). One main aim of any future work is to improve the modelling framework to account for the combined impacts of changes in climate forcing and expected changes in DOC and water clarity. These assumptions thus introduce uncertainties of the methodological and epistemological type (Funtowicz & Ravetz 1990; Saloranta

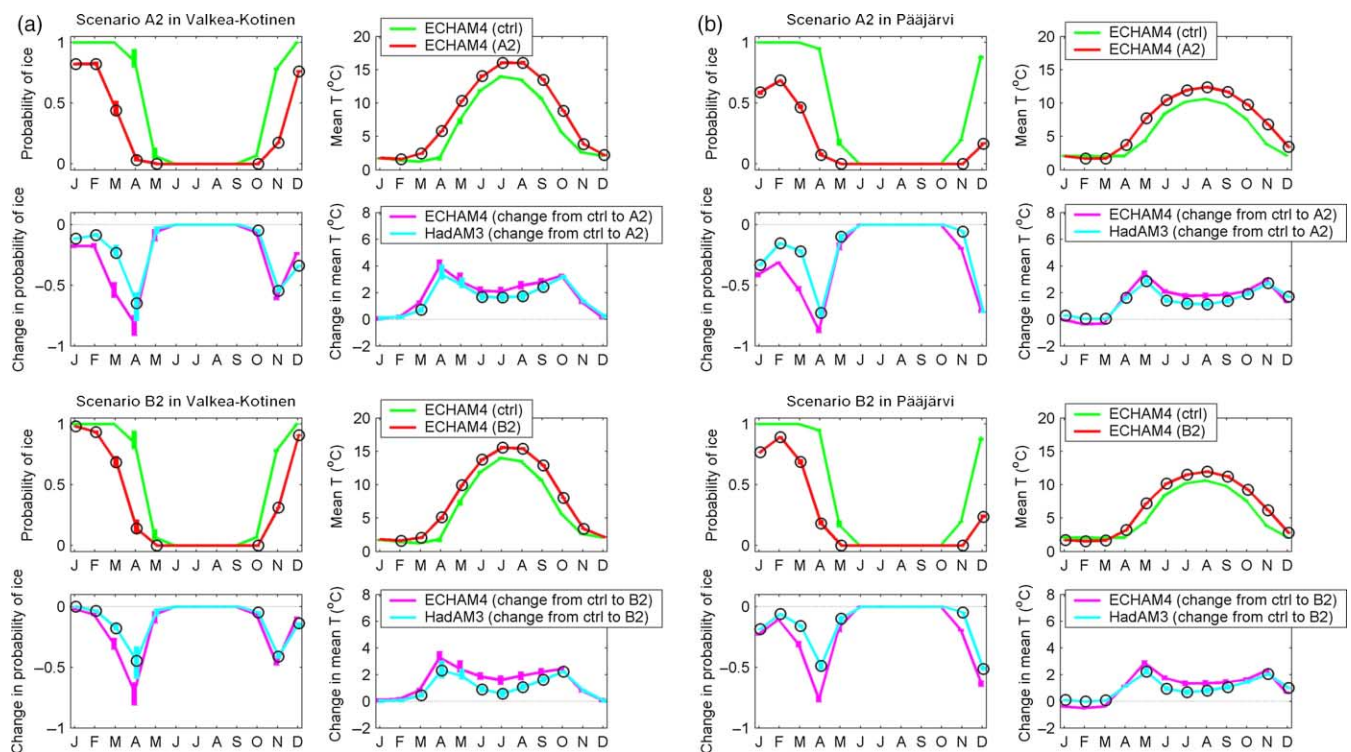


Figure 6 | Simulated monthly mean probability of ice cover and mean lake temperature in (a) Valkeakotinen and (b) Pääjärvi in the six different climate forcing scenarios, i.e. in control scenarios in 1961–1990 (denoted by light (green) lines for ECHAM4 forcing), as well as in scenarios A2 and B2 in 2071–2100 (denoted by dark (red) lines for ECHAM4 forcing). The first simulation years 1961 and 2071 are not included in the means. The corresponding difference between the control and scenarios A2 and B2 in simulations with both HadAM3 and ECHAM4 forcings are denoted by the light (blue) and dark (pink) lines. The thick solid lines denote the median and the vertical error bars the 90% credible intervals of the 200 simulations conducted in the uncertainty analysis, where parameter values sets were resampled from the parameter chain estimated in the MCMC simulation. The black rings denote months where with >90% probability there is a consistent difference between the two plotted scenarios (i.e. >90% of the 200 simulated values in one scenario are smaller/larger than in the other scenario).

et al. 2003) which the uncertainty analysis cannot quantitatively capture, i.e. uncertainties associated with how adequately the model code and equations represent the lake system functioning in the present and future climate, and with the current scientific understanding on the lake system processes in the present and future climate.

Figure 7 shows how the monthly mean increase in air temperature in the projected future climate is “translated” to epilimnion and whole lake water temperatures. In the period from April–May to October–November the water temperature change is roughly proportional to the air temperature change, while in winter and early spring there is in fact a negative correlation between the amount of change in water and air temperatures in a projected future climate. This feature is due to the buffering effect of ice cover, where warmer autumn and winter air temperatures only delay ice formation and affect the thickness of the ice but do not affect water temperatures significantly, since

autumn/winter monthly mean air temperatures are still not much above the water freezing point. In fact, the mean monthly air temperature is still lower than 4.0°C (the temperature of the maximum density of water) in all the four scenarios of future climate (ECHAM4 and HadAM3 forcings, A2 and B2 scenarios) in November–March, despite quite a large temperature increase compared to the control period. Due to the prolonged ice-free period in the autumn, the autumn turnover circulation is also prolonged, so that the increase in autumn/winter air temperature in the projected future climate can even produce a slight cooling effect in the whole lake mean temperature, as is the case in January–March in Pääjärvi.

In the spring, however, the thinner ice cover together with warmer air temperatures lead to earlier ice melting which produces the largest change in water temperatures in a projected future climate compared to the present climate. In other words, in the projected future climate, the increase

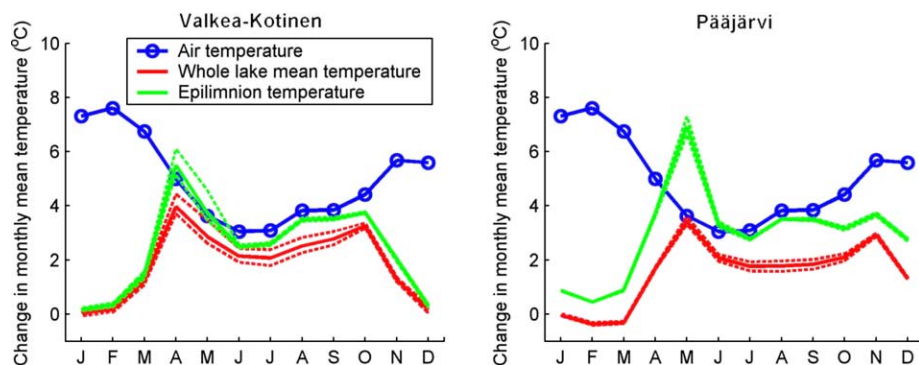


Figure 7 | Simulated change in monthly mean air, whole lake and epilimnion (0.5 m depth in (a) and 1 m depth in (b)) temperatures between control (1961–1990) and A2 (2071–2100) scenarios with the ECHAM4 forcing in (a) Valkea-Kotinen and (b) Pääjärvi. The first simulation years 1961 and 2071 are not included in the means. The thick solid lines denote the median and the dashed lines the 90% credible intervals of the 200 simulations conducted in the uncertainty analysis, where parameter values sets were resampled from the parameter chain estimated in the MCMC simulation.

in atmospheric heating in autumn/winter is accumulated and delayed until spring when it is finally manifested as the largest lake water temperature change.

The mean difference in air temperature between control and A2 scenarios with ECHAM4 forcing over the whole 29-year simulation period is 5.0°C and similarly the simulated difference in the epilimnion (0.5 or 1 m depths) and whole lake mean temperatures are 2.4 and 1.9°C in Valkea-Kotinen and 3.0 and 1.5°C in Pääjärvi (medians of the 200 long-term means calculated in the uncertainty analysis). Thus, of the 5.0°C increase in air temperature, on average 49% is translated to epilimnion and 37% to the whole lake water column in Valkea-Kotinen, while similar values are 59% and 30% in Pääjärvi. Due to the higher depth of Pääjärvi and the isolating effect of the pycnocline, which reduces the vertical mixing between the epi- and hypolimnion, the whole lake temperature change is smaller in Pääjärvi than in Valkea-Kotinen. Similarly, probably due to the larger size of Pääjärvi, and thus deeper pycnocline (i.e. deeper epilimnion), the ice-covered period is shortened more in Pääjärvi than in Valkea-Kotinen in the projected future climate, which leads to a slightly larger increase of yearly mean epilimnion temperature in Pääjärvi compared to Valkea-Kotinen.

Figure 7 demonstrates that the changes in atmospheric climate are not necessarily straightforwardly translated to changes in “lake water climate”. This is mainly due to the threshold-like buffering effect of the ice freezing and melting processes and the turnover mixing processes due to water maximum density at 4.0°C. Korhonen (2006) analyzed freeze-up and break-up records of almost 90

lakes dating back to the early 19th century, and ice thickness records of about 30 lakes dating back to the 1910s, in order to identify long-term changes in the ice regime in Finland (Pääjärvi and Valkea-Kotinen are not included in this analysis). This analysis showed a significant change towards earlier ice break-up in Finland, except in the very north, from the late 19th century to the present time. There was also a significant trend towards later freeze-up and thus also towards a shorter ice cover duration for the longest time series. However, somewhat surprisingly the ice thickness seems to have increased over the last 40 years (although there were significant trends only in half of the investigated lakes). This increased ice thickness is most likely due to heavy snow on the ice and production of snow ice.

Models together with proper model analysis techniques (calibration, uncertainty and sensitivity analysis) can provide an excellent way of better synthesizing these nonlinear processes and so better understanding the sometimes non-trivial impacts of changing climate on lake water thermodynamics.

In this paper, the physical lake system has been considered. Increased system complexity and some unexpected responses are likely to appear when the focus of attention is shifted to the question of how the changes in climate and water thermodynamics impact the lake chemistry and biology. This is illustrated in the results of the whole-lake manipulation experiment of Lydersen *et al.* (2008) who found surprisingly small changes in the chemistry and biology of an oligotrophic clear water lake

despite large changes in the lake thermodynamics. A similar whole-lake manipulation experiment was also conducted recently in Halsjärvi, a lake very similar to Valkea-Kotinen, and results from this experiment will provide us with more empirical knowledge on the potential climate change impacts on the chemistry and biology of lakes.

ACKNOWLEDGEMENTS

We warmly thank Patrick Samuelsson for providing the RCAO simulation results for our study and the three reviewers for their constructive comments on the manuscript. This study was funded by the Commission of European Communities, the Research Council of Norway and the Norwegian Institute for Water Research (Eurolimpacs project, GOCE-CT-2003-505540).

REFERENCES

- Arhonditsis, G. B., Qian, S. S., Stow, C. A., Lamon, E. C. & Reckhow, K. H. 2007 Eutrophication risk assessment using Bayesian calibration of process-based models: application to a mesotrophic lake. *Ecol. Modell.* **208**, 215–229.
- Beven, K. 2006 A manifesto for the equifinality thesis. *J. Hydrol.* **320**, 18–36.
- Blenckner, T. 2005 A conceptual model of climate-related effects on lake ecosystems. *Hydrobiologia* **533**, 1–14.
- Blenckner, T. 2008 Models as tools for understanding past, recent and future changes in large lakes. *Hydrobiologia* **599**, 177–182.
- Blenckner, T., Adrian, R., Livingstone, D. M., Jennings, E., Weyhenmeyer, G. A., George, D. G., Jankowski, T., Järvinen, M., NicAonghusa, C., Nöges, T., Straile, D. & Teubner, K. 2007 Large-scale climatic signatures in lakes across Europe: a meta-analysis. *Global Change Biol.* **13**, 1314–1326.
- Blenckner, T., Järvinen, M. & Weyhenmeyer, G. A. 2004 Atmospheric circulation and its impacts on ice phenology in Scandinavia. *Boreal Environ. Res.* **9**, 371–380.
- Blenckner, T., Omstedt, A. & Rummukainen, M. 2002 A Swedish case study of contemporary and possible future consequences of climate change on lake function. *Aquatic Sci.* **64**, 171–184.
- Fang, X. & Stefan, H. G. 1998 Potential climate warming effects on ice covers of small lakes in the contiguous U.S. *Cold Regions Sci. Technol.* **27**, 119–140.
- Forsius, M., Kleemola, S., Starr, M. & Ruoho-Airola, T. 1995 Ion mass budgets for small forested catchments in Finland. *Water Air Soil Pollut.* **79**, 19–38.
- Funtowicz, S. O. & Ravetz, J. 1990 *Uncertainty and Quality in Science for Policy*. Kluwer, Dordrecht.
- Futter, M. N., Forsius, M., Holmberg, M. & Starr, M. 2009 A long-term simulation of the effects of acidic deposition and climate change on surface water dissolved organic carbon concentrations in a boreal catchment. *Hydrol. Res.* **40**(2–3), 291–305.
- Gamerman, D. 1999 *Markov Chain Monte Carlo: Stochastic Simulation for Bayesian Inference*. Chapman & Hall, London.
- Gelman, A., Carlin, B. C., Stern, H. S. & Rubin, D. B. 2004 *Bayesian Data Analysis*, 2nd edition. Chapman & Hall, London.
- George, D. G., Järvinen, M. & Arvola, L. 2004 The influence of the North Atlantic Oscillation on the winter characteristics of Windermere (UK) and Pääjärvi (Finland). *Boreal Environ. Res.* **9**, 389–399.
- Haario, H., Saksman, E. & Tamminen, J. 2001 An adaptive Metropolis algorithm. *Bernoulli* **7**, 223–242.
- Henneman, H. E. & Stefan, H. G. 1999 Albedo models for snow and ice on a freshwater lake. *Cold Regions Sci. Technol.* **29**, 31–48.
- Holmberg, M., Forsius, M., Starr, M. & Huttunen, M. 2006 An application of artificial neural networks to carbon, nitrogen and phosphorus concentrations in three boreal streams and impacts of climate change. *Ecol. Modell.* **195**, 51–60.
- Hondzo, M. & Stefan, H. G. 1993 Lake water temperature simulation model. *J. Hydraul. Engng.* **119**, 1251–1273.
- Hostetler, S. W. & Small, E. E. 1999 Response of North American freshwater lakes to simulated future climates. *J. AWRA* **35**, 1625–1637.
- IPCC (Intergovernmental Panel on Climate Change) 2001 (ed, Houghton, J. T., et al.), *Climate Change 2001: The Scientific Basis*. Cambridge University Press, Cambridge.
- Järvinen, M., Lehtinen, S. & Arvola, L. 2006 Variations in phytoplankton assemblage in relation to environmental and climatic variation in a boreal lake. *Verh. Int. Verein. Limnol.* **29**, 1841–1844.
- Järvinen, M., Rask, M., Ruuhijärvi, J. & Arvola, L. 2002 Temporal coherence in water temperature and chemistry under the ice of boreal lakes (Finland). *Water Res.* **36**, 3949–3956.
- Jones, C. G., Willén, U., Ullerstig, A. & Hansson, U. 2004 The Rossby centre regional atmospheric climate model part I: model climatology and performance for the present climate over Europe. *Ambio* **33**, 199–210.
- Kankaala, P., Arvola, L., Tulonen, T. & Ojala, A. 1996 Carbon budget for the pelagic food web of the euphotic zone in a boreal lake (Lake Pääjärvi). *Can. J. Fish. Aquatic Sci.* **53**, 1663–1674.
- Kankaala, P., Huotari, J., Peltomaa, E., Saloranta, T. & Ojala, A. 2006 Methanotrophic activity in relation to methane efflux and total heterotrophic bacterial production in a stratified, humic, boreal lake. *Limnol. Oceanogr.* **51**, 1195–1204.
- Keskitalo, J., Salonen, K. & Holopainen, A.-L. 1998 Long-term fluctuations in environmental conditions, plankton and macrophytes in a humic lake, Valkea-Kotinen. *Boreal Environ. Res.* **3**, 251–262.

- Korhonen, J. 2006 Long-term changes in lake ice cover in Finland. *Nordic Hydrol.* **37**, 347–363.
- Kuczera, G. & Parent, E. 1998 Monte Carlo assessment of parameter uncertainty in conceptual catchment models: the Metropolis algorithm. *J. Hydrol.* **211**, 69–85.
- Larssen, T., Huseby, R. B., Cosby, B. J., Høst, G., Høgåsen, T. & Aldrin, M. 2006 Forecasting acidification effects using a Bayesian calibration and uncertainty propagation approach. *Environ. Sci. Technol.* **40**, 7841–7847.
- Leppäranta, M., Reinart, A., Erm, A., Arst, H., Hussainov, M. & Sipelgas, L. 2003 Investigation of ice and water properties and under-ice light fields in fresh and brackish water bodies. *Nordic Hydrol.* **34**, 245–266.
- Livingstone, D. M. & Dokulil, M. T. 2001 Eighty years of spatially coherent Austrian lake surface temperatures and their relationship to regional air temperature and the North Atlantic Oscillation. *Limnol. Oceanogr.* **46**, 1220–1227.
- Lydersen, E., Aanes, K. J., Andersen, S., Andersen, T., Brettum, P., Bækken, T., Lien, L., Lindstrøm, E. A., Løvik, J. E., Mjelde, M., Oredalen, T. J., Solheim, A. L., Romstad, R. & Wright, R. F. 2008 Ecosystem effects of thermal manipulation of a whole lake, lake Breisjøen, southern Norway (THERMOS project). *Hydrol. Earth Syst. Sci.* **12**, 509–522.
- Malve, O., Laine, M. & Haario, H. 2005 Estimation of winter respiration rates and prediction of oxygen regime in a lake using Bayesian inference. *Ecol. Modell.* **182**, 183–197.
- Malve, O., Laine, M., Haario, H., Kirkkala, T. & Sarvala, J. 2007 Bayesian modelling of algal occurrences - using adaptive MCMC methods with a lake water quality model. *Environ. Modell. Software* **22**, 966–977.
- Monteith, D. T., Stoddard, J. L., Evans, C. D., de Wit, H. A., Forsius, M., Høgåsen, T., Wilander, A., Skjelkvåle, B. L., Jeffries, D. S., Vuorenmaa, J., Keller, B., Kopacek, J. & Vesely, J. 2007 Dissolved organic carbon trends resulting from changes in atmospheric deposition chemistry. *Nature* **450**, 537–539.
- Perovich, D. 1998 The optical properties of sea ice. In: Leppäranta, M. (ed.) *Physics of Ice-covered Seas*. Helsinki University Printing House, Helsinki, Finland, pp. 195–230.
- Räisänen, J., Hansson, U., Ullerstig, A., Döscher, R., Graham, L. P., Jones, C., Meier, H. E. M., Samuelsson, P. & Willén, U. 2004 European climate in the late twenty-first century: regional simulations with two driving global models and two forcing scenarios. *Climate Dyn.* **22**, 13–31.
- Rask, M., Holopainen, A.-L., Karusalmi, A., Niinioja, R., Tammi, J., Arvola, L., Keskitalo, J., Blomqvist, I., Heinimaa, S., Karppinen, C., Salonen, K. & Sarvala, J. 1998 An introduction to the limnology of the Finnish Integrated Monitoring lakes. *Boreal Environ. Res.* **3**, 263–274.
- Salonen, K., Jones, R. I. & Arvola, L. 1984 Hypolimnetic phosphorus retrieval by diel vertical migrations of lake phytoplankton. *Freshwater Biol.* **14**, 431–438.
- Saloranta, T. M. 2006 Highlighting the model code selection and application process in policy-relevant water quality modelling. *Ecol. Modell.* **194**, 316–327.
- Saloranta, T. M. & Andersen, T. 2007 MyLake—a multi-year lake simulation model suitable for uncertainty and sensitivity analysis simulations. *Ecol. Modell.* **207**, 45–60.
- Saloranta, T. M., Armitage, J. M., Haario, H., Næs, K., Cousins, I. T. & Barton, D. N. 2008 Modeling the effects and uncertainties of contaminated sediment remediation scenarios in a Norwegian fjord by Markov chain Monte Carlo simulation. *Environ. Sci. Technol.* **42**, 200–206.
- Saloranta, T. M., Kämäri, J., Rekolainen, S. & Malve, O. 2003 Benchmark criteria: a tool for selecting appropriate models in the field of water management. *Environ. Mngmnt.* **32**, 322–333.
- Saltelli, A., Chan, K. & Scott, E. M. 2000 *Sensitivity Analysis*. Wiley, New York.
- Starr, M. & Ukonmaanaho, L. 2001 Results from the first round of the integrated monitoring soil chemistry subprogramme. In: Ukonmaanaho, L. & Raitio, H. (eds) *Forest Condition in Finland. National Report 2000*. Research Papers 824. Finnish Forest Research Institute, Helsinki, pp. 140–157.
- Starr, M. & Ukonmaanaho, L. 2004 Levels and characteristics of TOC in throughfall, forest floor leachate and soil solution in undisturbed boreal forest ecosystems. *Water Air Soil Pollut. Focus* **4**, 715–729.
- Vähätalo, A. V., Salkinoja-Salonen, M., Taalas, P. & Salonen, K. 2000 Spectrum of the quantum yield for photochemical mineralization of dissolved organic carbon in a humic lake. *Limnol. Oceanogr.* **45**, 664–676.
- Vähätalo, A. V., Salonen, K., Münster, U., Järvinen, M. & Wetzel, R. G. 2003 Photochemical transformation of allochthonous organic matter provides bioavailable nutrients in a humic lake. *Arch. Hydrobiol.* **156**, 287–314.
- Weyhenmayer, G. A., Westö, A.-K. & Willen, E. 2008 Increasingly ice-free winters and their effects on water quality in Sweden's largest lakes. *Hydrobiologia* **599**, 111–118.

First received 17 April 2008; accepted in revised form 30 January 2009